Biorecognition of HPMA Copolymer-Adriamycin Conjugates by Lymphocytes Mediated by Synthetic Receptor Binding Epitopes

Vladimir Omelyanenko,[1] Pavla Kopečková,[1] Ramesh K. Prakash,[2] Charles D. Ebert[2], and Jindřich Kopeček[1,3]

Received January 27, 1999; accepted March 23, 1999

Purpose. The EDPGFFNVE nonapeptide (NP) was recognized as the CD21 (CR2) binding epitope of the Epstein-Barr virus (EBV) gp350/220 envelope glycoprotein which mediates the virus attachment to human B lymphocytes (Nemerow *et al.*, Cell 56:369-377, 1989). Here we evaluated the targeting potential of a synthetic receptor binding epitope (NP) covalently attached to a water-soluble polymeric drug carrier. In particular, the biorecognition of N-(2-hydroxypropyl)methacrylamide (HPMA) copolymer-NP conjugates by B- and T-cells and the cytotoxicity of HPMA copolymer-NP-adriamycin (ADR) conjugates toward B-cells, T-cells, and peripheral blood lymphocytes (PBL) were evaluated.

Methods. HPMA copolymer-NP and optionally ADR conjugates varying in the NP density and mode of NP attachment were incubated with Raji B-cells (human Burkitt's lymphoma), CCRF-CEM T-cells (acute human lymphoblastic leukemia), and CCRF-HSB-2 T-cells (human lymphoblastic leukemia). The kinetics of binding was studied, the Langmuir adsorption isotherms analyzed, binding constants calculated, and IC_{50} doses determined.

Results. Flow cytometry studies revealed that binding was homogeneous to both cell types. The apparent binding constants to T-cells were about two times higher when compared to B-cells. The binding and cytotoxicity increased with increased amount of epitopes per polymer chain. Attachment of the NP via a GFLG spacer resulted in increased biorecognition when compared with conjugates containing NP bound via a GG spacer. HPMA copolymer-NP-ADR conjugates possessed specific cytotoxicity to T- and B-malignant cells. Concentrations, which were lethal to the latter, were not toxic for PBL.

Conclusions. The data obtained seem to indicate the potential of the HPMA copolymer-NP conjugates as polymer anticancer drug carriers targetable to immunocompetent cells.

KEY WORDS: T-cells; B-cells; HPMA copolymer; drug carrier; targeting; cancer therapy; CD21 receptor; adriamycin; doxorubicin.

INTRODUCTION

The use of polymeric drug delivery systems is rapidly becoming an established approach for improvement of cancer chemotherapy. The covalent binding of low molecular weight drugs to water soluble polymer carriers offers a potential mechanism to enhance the specificity of drug action. Endocytosis becomes the only mode of cell entry of drug-polymer conjugates; this can be a highly cell specific mechanism (1,2).

During the last decade we have designed, developed, and evaluated targetable N-(2-hydroxypropyl)methacrylamide (HPMA) copolymer-anticancer drug conjugates (reviewed in part 5 of ref. 1). Various targeting moieties, such as carbohydrates (3) and antibodies (4,5) have been used to achieve the biorecognizability of these conjugates. One of the main advantages is the possibility of attaching numerous biorecognizable moieties to one macromolecule. The biorecognition of HPMA copolymers containing side-chains terminated in N-acylated galactosamine by the asialoglycoprotein receptor was dependent on the amount of bound ligand (3). Similar advantage of multivalent interactions (cooperative binding) was observed in the inhibition of virus mediated agglutination of erythrocytes by polyacrylamides with pendant sialoside groups (6), lectin recognition of HPMA copolymers with pendant fucosylamine residues (7), and BCL_1 mouse lymphoma binding of short peptides fused via a semi-rigid hinge region with the coiled-coil assembly domains into a multivalent binding molecule (8).

Another advantage of macromolecular carriers containing multiple small epitopes may be in the easier transcompartmental transport when compared to large antibody conjugates. It is well established that increased permeability of tumor vasculature combined with impaired lymphatic drainage results in the accumulation of macromolecules in tumor tissue (3). Other factors, however, may have an opposite effect. For example, a high interstitial pressure may result in a convective fluid flow from the center of the tumor to the periphery which might carry macromolecules (9). Nevertheless, increased concentrations of HPMA copolymer bound drugs (when compared to free drugs) were observed on several tumor models (10,11). It appears that the permeability and accessibility of a particular tumor will depend on many factors, one of the very important ones being the size of the macromolecule. It was recently demonstrated that the effective permeability of small macromolecules, such as albumin was independent of the tumor pore cutoff size (12). HPMA copolymers used as drug carriers possess a small size (< 10 nm). However, this advantage is relevant mainly to the treatment of solid tumors.

The Epstein-Barr virus (EBV) gp350/220 envelope glycoprotein mediates virus attachment to the EBV/C3dg receptor on human B lymphocytes (13) and specific binding to some receptors on human T cell lymphomas (14). Two regions of amino acid similarity were found in the gp350 and C3d coding sequences and it was suggested that they may represent CD21 (CR2) binding sites of gp350/220. It was shown that multimeric forms of the N-terminal gp350/220 peptide, composed from nine amino acid residues (EDPGFFNVE), conjugated to albumin efficiently blocked recombinant gp350/220 and C3dg binding to B cells (13).

In this study the potential of the covalently attached EDPGFFNVE nonapeptide (NP) as a targeting moiety for HPMA

[1] Department of Pharmaceutics and Pharmaceutical Chemistry, University of Utah, Salt Lake City, Utah 84112.

[2] TheraThech, Inc., Salt Lake City, Utah 84108.

[3] To whom correspondence should be addressed. (e-mail: jindrich.kopecek@m.cc.utah.edu)

ABBREVIATIONS: AIBN, 2,2′-azobisisobutyronitrile; ADR, adriamycin (doxorubicin); CB, Cascade Blue; DPBS, Dulbecco's phosphate buffered saline; EBV, Epstein-Barr virus; FBS, fetal bovine serum; HPMA, N-(2-hydroxypropyl) methacrylamide; NP, nonapeptide EDPGFFNVE; MA-GFLG-ONp, N-methacryloylglycylphenylalanylleucylglycine p-nitrophenyl ester; MA-GG-ONp, N-methacryloylglycylglycine p-nitrophenyl ester; ONp, p-nitrophenoxy; P, HPMA copolymer backbone; PBL, peripheral blood lymphocytes.

0724-8741/99/0700-1010$16.00/0

copolymers has been evaluated. The biorecognition of the HPMA copolymer-NP conjugates by B- and T-lymphocytes was studied. The NP was attached to the HPMA copolymer backbone via dipeptide (GG) or tetrapeptide (GFLG) side-chains (15), and covalently attached Cascade Blue (CB) was used as the fluorescence marker of the conjugate. The content of NP containing side-chains was varied to determine the impact of the cooperativity effect on biorecognition. The cytotoxicity of HPMA copolymer-ADR-NP conjugates toward CCRF-CEM and CCRF-HSB-2 T-cell lines, Raji B-cell line, and human PBL was determined.

MATERIALS AND METHODS

Materials

RPMI 1640 medium, Iscove's modified medium, penicillin/streptomycin stock solution and Dulbecco's phosphate buffered saline (DPBS) were obtained from Sigma Chemical Co. (St. Louis, MO). Fetal bovine serum (FBS) was from HyClone (Logan, UT). Sephadex G-25 (PD-10) columns and a Superose 6 (16/60) column were from Pharmacia (Piscataway, NJ). Cascade Blue was from Molecular Probes (Eugene, OR). The ADR was a kind gift from Dr. A. Suarato, Pharmacia-Upjohn (Milano, Italy). Deionized water was used for the preparation of all buffers. All other chemicals were of reagent grade or better.

Cell Lines

Raji B-cell line (Burkitt's lymphoma, human), CCRF-CEM T-cell line (acute lymphoblastic leukemia, human), and CCRF-HSB-2 T-cell line (lymphoblastic leukemia) were obtained from the American Type Culture Collection (ATCC, Rockville, Maryland). Raji and CCRF-CEM cells were cultured in RPMI medium supplemented subsequently with 10% and 20% FBS. CCRF-HSB-2 cell were cultured in Iscove's modified medium supplemented with 10% FBS. All media contained penicillin (100 U/ml), and streptomycin (100 μg/ml). Cells were grown at 37°C in a humidified atmosphere of 5% CO_2 (v/v) in air. Cell density in a culture was kept at 0.5–1 × 10^6 cells per ml of medium.

HPMA Copolymer-NP Conjugates

The conjugates were synthesized using a two step procedure. In the first step, the polymer precursors were prepared by radical precipitation copolymerization of HPMA and N-methacryloylglycylphenylalanylleucylglycine p-nitrophenyl ester or N-methacryloylglycylglycine p-nitrophenyl ester (16). Two polymer precursors were prepared: one contained 8.7 mol% glycylphenylalanylleucylglycine p-nitrophenyl ester side chains (M_w = 20500; M_w/M_n = 1.4), the other 9.5 mol% glycylglycine p-nitrophenyl ester side chains (M_w = 19400; M_w/M_n = 1.4). The fluorescent marker, Cascade Blue (CB) or adriamycin (ADR) and the nonapeptide (NP; EDPGFFNVE) were bound to polymer precursors by consecutive aminolysis of reactive ester groups (17) without isolation of the intermediate product. The synthesis of conjugate **1** containing NP and CB and the synthesis of conjugate **4** containing NP and ADR are described as examples.

Synthesis of P(GFLG)-NP-CB (1)

To a stirred solution of 300 mg polymer precursor (8.7 mol%-GFLG-ONp; 145 μmol ONp groups) in 1.5 ml DMF a suspension of CB (20 mg; 30 μmol) in 0.5 ml DMF was added. Within 30 min the reaction mixture cleared up and then the NP (126 mg; 120 μmol) was added followed by slow addition of 70 μl (505 μmol) triethylamine. After 5 h stirring at room temperature the polymer was precipitated into an excess of acetone, filtered off and dried. The conjugate was then extensively dialyzed from an aqueous solution and isolated by freeze drying. The content of bound NP was determined by amino acid analysis, the content of bound CB was determined spectrophotometrically using extinction coefficient 2.9 × 10^4 M^{-1} cm^{-1} (λ_{max}, 400 nm in borate buffer pH 9.2). The absence of non-bound ligands was checked by SEC using UV detection at 280 nm. The yield of conjugate after freeze drying was 290 mg; the content of NP was 20.8 wt.% and the content of CB 3.8 wt.%

Synthesis of P(GFLG)-NP-ADR (4)

To a suspension of 300 mg polymer precursor (145 μmol ONp), 36 mg (62 μmol) ADR.HCl and 30 mg (28 μmol) NP in 2.0 ml DMF, 41 μl (292 μmol) triethylamine (diluted 1:1 in DMF) were slowly added. The reaction mixture was stirred in the dark for 5 h at room temperature. Then 20 μl of 1-amino-2-propanol was added to aminolyze non-reacted ONp goups and the copolymer was immediately precipitated into acetone/ether (3:1), washed, and dried. The polymer was purified by Sephadex LH-20 chromatography in MeOH containing 10% DMSO and 1% CH_3COOH followed by dialysis. After freeze drying the polymer was characterized by the determination of bound NP (amino acid analysis) and by the content of bound ADR (ε = 11000 $M^{-1}cm^{-1}$ in H_2O; λ 485 nm).

The synthesis of other polymer conjugates was performed similarly to that described for conjugates **1** and **4**. The HPMA copolymer conjugates containing the tetrapeptide (GFLG) spacer are referred to as P(GFLG)- and those containing the dipeptide (GG) spacer are referred to as P(GG)-, where P is the HPMA copolymer backbone. The structures and composition of the conjugates are shown in Fig. 1. The amount of NP, CB, and ADR in mol-% is very close to the actual number of NP, CB, and ADR per one polymer chain. The M_w of polymer conjugates **1**–**8** were ⟨19,500–25,000⟩.

Binding Assays

Kinetics

Cells were transferred from a culture medium into DPBS containing 30 mM NaN_3 and 0.5% of BSA, placed in Eppendorf vials (1 × 10^6 cells in 250 μl), and chilled to 0°C for 30 min. Conjugates P(GFLG)-NP-CB (**1**) and P(GG)-CB (**8**, control) in DPBS (2 mg/ml) at 0°C were added to cell suspensions at final concentration 400 μg/ml and the cells incubated for various time intervals at 0°C. The cells were spun down at 14,000 rpm in a microrotor of the Biofuge 14R centrifuge for 30 min. The supernatant containing unbound conjugates was carefully removed and the cell pellet dissolved in 1 M NaOH overnight. The amount of the bound conjugate was determined by fluorescence spectrophotometry and the cell protein content by the

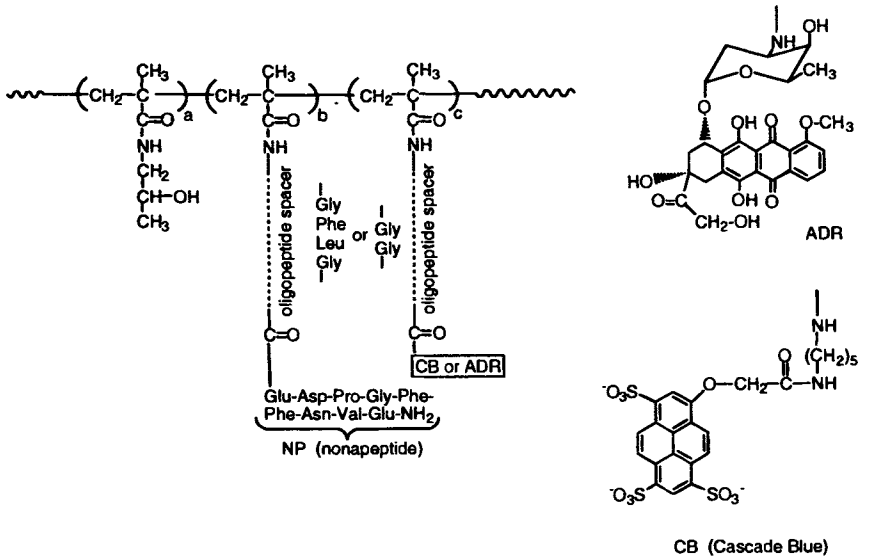

Conjugate No.	Spacer	a	b (mol %)	c	NP	CB (wt.%)	ADR
1	GFLG	95.0	3.9	1.1 (CB)	20.8 ("high" NP)	3.8	-
2	GFLG	97.0	1.2	1.8 (CB)	6.8 ("low" NP)	6.5	-
3	GFLG	94.1	3.5	2.4 (ADR)	17.2 ("high" NP)	-	7.3
4	GFLG	96.2	1.2	2.6 (ADR)	6.0 ("low" NP)	-	8.0
5	GFLG	96.8	3.2	-	18.1	-	-
6	GFLG	98.1	-	1.9 (ADR)	-	-	6.1
7	GG	93.0	5.6	1.4 (CB)	28.5	4.6	-
8	GG	98.1	-	1.9 (CB)	-	8.1	-

Fig. 1. Structures and composition of conjugates.

Lowry assay. The amount of P(GFLG)-NP-CB conjugate bound to the cell surface was determined as

$$C_{bound} = (F_{NP} - F_{control})/F_{standard} \quad (1)$$

where F_{NP} is the fluorescence of the cells (dissolved cell pellet) incubated with P(GFLG)-NP-CB (average value from three vials and normalized per the cell proteins). The $F_{control}$ is the fluorescence of cells (dissolved cell pellet) incubated with the P(GG)-CB conjugate, i.e., the fluorescence of conjugate trapped by cells during centrifugation (average value from three vials and normalized per the cell proteins). The $F_{standard}$ is the fluorescence of a known amount of P(GFLG)-CB dissolved in 1 M NaOH.

Langmuir Adsorption Isotherms

Various concentrations of conjugates were added to cells in DPBS (containing 30 mM NaN_3 and 0.5% BSA) at 0°C and incubated for 4 h to reach equilibrium. The P(GG)-CB (**8**) was used as a control conjugate to estimate the amount of conjugates trapped with cells during the cell spinning. The Langmuir binding isotherms of conjugates normalized per 1×10^6 cells were analyzed. The parameters of binding, K_a (affininty constant) and R (total amount of receptors) were estimated by fitting experimental data with the equation:

$$C_{bound} = K_a \cdot R \cdot C_{free}/(1 + K_a \cdot C_{free}) + \alpha C_{free} \quad (2)$$

The amount of free conjugates in solution – C_{free} was calculated as $C_{free} = C_{added} - C_{bound}$, where C_{added} is the concentration of conjugates added to the cell suspension, and α the parameter corresponding to nonspecific interactions of conjugates with the cell surface. The α values were determined independently in experiments where receptors were saturated with conjugates (0.5 mM of NP equivalent). Average values of C_{bound} from three measurements were used to construct the Langmuir isotherm plots.

Confocal Fluorescence Microscopy Study of P(GFLG)-NP-ADR Internalization

A Bio-Rad MRC 600 laser scanning confocal imaging system based on a Zeis Axioplan microscope and a krypton/argon laser was employed to observe internalization of the targeted conjugate. A planapo objective (×60, numerical aperture 1.4, oil) was used. The ADR fluorescence images were accumulated via the BHS block of filters (excitation at 488 nm and emission through a 515 nm barrier filter). Cells were cultured with P(GFLG)-NP-ADR conjugates at concentration 100 μg/ml (12 μM of ADR) for 24 h. After incubation the cells were washed three times with PBS, transferred on polylysine treated glass coverslips, and kept in PBS for 20 min at 4°C. Cells were fixed with 1% paraformaldehyde for 10 min at 4°C and rinsed with PBS. Inverted coverslips were mounted on glass slides in 50% glycerol and 0.02% NaN_3. The slides were examined immediately. In all cases, the operating conditions

were such that detectable images could not be obtained for cell samples not treated by the conjugate.

Cytotoxicity Assays

Cytotoxicity

The cytotoxicity of drugs was assessed using a modified MTT (3-(4,5-dimethylthiazol-2-yl)-2,5-diphenyltetrazolium bromide) assay (18). Briefly, cells were seeded into 96-well microtiter plates at the density of 10,000 cells per well. Twenty-four hours after plating, the medium was aspirated and 12 different concentrations (expressed as ADR equivalents) of sterile HPMA copolymer conjugates in fresh media were added. Cells were cultured for 72 h with the conjugates before the cell survival assay was performed. The medium was discarded and 100 μl of fresh medium plus 25 μl of a 5 mg/ml MTT (Fluka) solution was added to each well. Plates were incubated under cell culture conditions for 3 h. Formazan crystals were dissolved overnight in 50% v/v dimethylformamide in water containing 20% w/v sodium dodecyl sulfate. The absorbance of each sample was measured at 570 nm with a background correction at 630 nm. The results of the cytotoxicity assay were used for the calculation of the IC_{50} dose (drug concentration which inhibits growth by 50% relative to non-treated control cells).

The cytotoxicity of the conjugates for PBL (obtained from a healthy donor) was assessed by flow cytometer analysis (FACS Scan, Becton Dickinson). The cells were separated by the Ficoll-Paque (Pharmacia) density gradient centrifugation, transferred into RPMI medium supplemented with 10% of FCS, and equal volumes placed into several wells of the 24-well plate. Various concentrations of conjugates (expressed in ADR equivalent) in sterile DPBS were added and cells cultured for 72 h at 37°C. Only DPBS was added to control cells. The cells were centrifuged, transferred into DPBS (0.5 ml) and analyzed in a flow cytometer. The lymphocytes were gated by their 'scatter morphology' (19). The accumulation of data continued till counting of the gated cells reached an adequate statistic. The time interval of counting was fixed and used as an interval of counting of the treated cells. Cell viability was calculated from the amount of treated cells possessing light scatter parameters typical for control cells and the amount obtained for control untreated cells.

Accumulation of HPMA Copolymer Conjugate in Subpopulations of PBL

Freshly obtained PBL cells were transferred into RPMI medium supplemented with 10% of FCS. The P(GFLG)-NP-CB conjugate (1) was added to the cells at a final concentration 100 μg/ml and the cells incubated for 72 h at 37°C. After incubation cells were divided into three portions. Each portion of cells was stained with a commercial antibody complementary for a receptor associated with a particular lymphocyte subpopulation. The Quantum Red™ conjugated mouse anti-human CD19 (Sigma) antibody was used to stain B lymphocytes. The FITC conjugated mouse monoclonal anti-human CD3 antibody (Sigma) was used to stain T lymphocytes. The FITC conjugated mouse anti-human CD4 (Sigma) was used to stain helper/inducer T lymphocytes. Cells were stained according to the procedure developed by the manufacturer. For negative staining controls, the isotype-matched non-specific mouse immunoglobulins conjugated with FITC or Quantum Red™ were used. Stained cells were immediately evaluated by flow cytometer analysis. Lymphocytes were gated by their 'scatter morphology'. Fluorescence intensity of CB was assumed to be proportional to the accumulation/association of the P(GFLG)-CB-NP conjugate in the subpopulation of lymphocytes.

Apoptosis Detection

The ApoAlert™ Annexin V/PI kit was used to monitor the early stage of apoptosis (Clontech, Palo Alto). The kit is based on staining of phosphatidylserine (PS); in apoptotic cells PS is translocated from the inner to the outer leaflet of the plasma membrane, thereby exposing PS to the external cellular environment (20). Cells were incubated with conjugates for 72 h at 37°C. Aliquots of cell suspension (about 10^4–10^5 cells) were withdrawn and washed with DPBS. The pellet of cells was resuspended in 200 μl of the binding buffer, 5 μl of Annexin V-FITC were added and cells incubated 15 min at room temperature. The cells were washed with DPBS (2 ml), resuspended in 0.5 ml of DPBS and immediately analyzed on a flow cytometer. Integrity of the cell membrane was controlled by staining of cells with Propidium Iodide (PI). To avoid spilling of the green fluorescence (FITC) to the red channel (PI) cells were stained with Annexin V-FITC and PI separately. The procedure of staining cells with PI was similar to staining cells with Annexin V-FITC. The plasma membrane integrity of cells exposed to ADR was controlled with Trypan Blue (samples where a completed compensation of ADR fluorescence in PI channel was limited).

RESULTS

Kinetics of Binding

Raji B-cells and HSB-2 T-cells were incubated with P(GFLG)-NP-CB conjugates for various periods of time at conditions where no cell internalization occurs (0°C in DPBS, 30 mM NaN_3, 0.5% BSA). Unbound conjugates were separated by centrifugation. Cells were spun and the cell pellet used to analyze the amount of bound conjugates by fluorescence spectrophotometry. The fluorescence intensity obtained from cells incubated with P(GG)-CB (at a concentration equal to the P(GFLG)-NP-CB conjugate) and separated from the incubation buffer by centrifugation, was used to estimate the amount of the trapped P(GFLG)-NP-CB conjugate. At neutral pH the P(GG)-CB conjugate is negatively charged. Consequently, it was reasonable to assume that its adsorption to the cell surface will be negligible. The kinetics of P(GFLG)-NP-CB binding (data not shown) demonstrated that in approximately 3 h an equilibrium was reached for both, Raji B-cells and HSB-2 T-cells.

Homogeneity of Cellular Biorecognition

Flow cytometric analysis was used to examine the homogeneity of the binding of P(GFLG)-NP-CB conjugate **1** to cells (Fig. 2). It appears that the whole population of Raji B-cells (Fig. 2A) and HSB-2 T-cells (Fig. 2B) were stained with the conjugate. These data indicated that the binding of conjugates

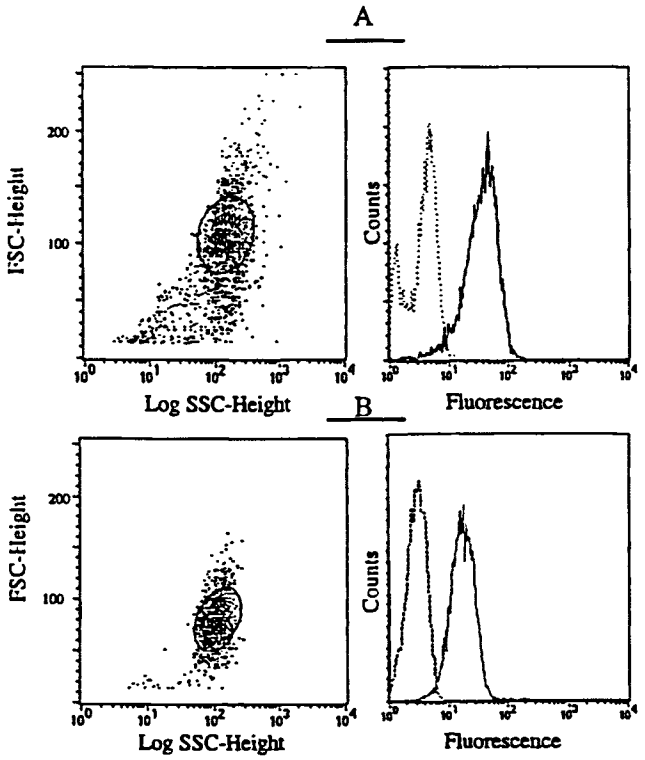

Fig. 2. Flow cytometric analysis of binding of the P(GFLG)-CB-NP conjugate **1** to Raji B-cells—upper two panels (A) and to CCRF-HSB-2 T-cells—lower two panels (B). Before analysis, cells were incubated with conjugate **1** for 4 h at 0°C.

to the cell surface can be normalized per cell number, for example 1×10^6.

Langmuir Isotherms

Both the binding efficacy and the amount of P(GFLG)-NP-CB conjugates bound to the cell surface of Raji B-cells, HSB-2 T-cells, and CCRF-CEM T-cells were estimated. Conditions of incubation (4 h, 0°C, 30 mM NaN_3) were chosen where no internalization occurred and receptor binding reached equilibrium. The character of the Langmuir adsorption isotherm plots indicated that P(GFLG)-NP-CB conjugate bound specifically to all three cell types used. The binding of the P(GFLG)-NP-CB conjugate was close to saturation at a concentration of conjugate corresponding to 50 μM of NP equivalent (Fig. 3).

To determine nonspecific binding, cells were incubated with P(GFLG)-NP at concentrations equal to 200 μM of NP equivalent to saturate the receptors. Then different concentrations of P(GFLG)-NP-CB conjugate were added and adsorption determined. The intensity of nonspecific binding of the conjugates was considerably lower when compared to specific binding (Fig. 3). The nonspecific adsorption data were approximated with a linear dependence and the parameter α (see Eq. 2). The parameter α for Raji B-cells was 1.5 fold higher than for HSB-2 T-cells. Apparently, this difference reflects the different size of the cells. Using an optical image analyzing software (Image-Pro) we found that an average diameter of Raji B-cells is 1.3–1.5 larger than the diameter of HSB-2 T-cells. This is in agreement with small angle light scattering data (14).

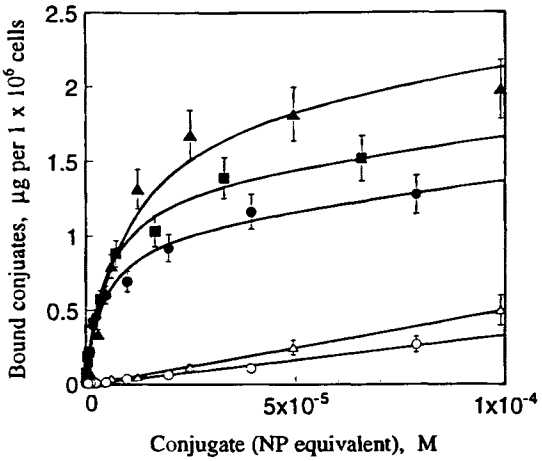

Fig. 3. Langmuir isotherm of the binding of the P(GFLG)-CB-NP conjugate **1** to Raji B-cells (▲), CCRF-HSB-2 T-cells (■), and CCRF-CEM T-cells (●). Non-specific adsorption of the conjugate to Raji B-cells (△) and CCRF-HSB-2 T-cells (○) is also shown. Cells were incubated with conjugate **1** for 4 h at 0°C. Solid lines are theoretical curves obtained by fitting of data with equation 2. Data of non-specific adsorption were approximated with a linear dependence.

Experimental data were fitted with equation 2 to calculate the affinity constant K_a and the amount of receptors per 1×10^6 cells (Table 1). Values of α parameters were fixed during the fitting procedure and NP ligands were treated as free ligands, interacting with receptors independently. Solid lines in Fig. 3 are theoretical curves obtained with calculated parameters.

Values of K_a were different for Raji B-cells and HSB-2 T-cells (Table 1). In the case of HSB-2 T-cells K_a was almost twice higher when compared to B-cells. K_a values for CEM and HSB-2 cells were very close. Differences in the values of the R parameter resulted probably from differences in the cell surface area. The data obtained are different from those published on binding of albumin and microspheres modified by the NP to B- and T-cells. Nemerow et al. observed NP mediated binding to B (Raji) cells and not to T (HSB-2) cells (13). We observed a higher affinity of the HPMA copolymer-NP

Table 1. Parameters[a] of Binding of HPMA Copolymer-CB-NP Conjugates to B- and T-Cells

Cells	Conjugate	K_a M × 10^5	R μg per 1 × 10^6 cells	α
Raji B-cells	**1**	1 ± 0.3	1.9 ± 0.3	5050
Raji B-cells	**2**	0.1 ± 0.07	2.0 ± 0.5	3000 ± 1500
Raji B-cells	**7**	0.2 ± 0.05	2.0 ± 0.3	1500 ± 1000
CCRF-HSB-2 T-cells	**1**	2.3 ± 0.2	1.0 ± 0.2	3360
CCRF-HSB-2 T-cells	**2**	0.2 ± 0.06	1.2 ± 0.3	2000 ± 1000
CCRF-HSB-2 T-cells	**7**	0.5 ± 0.1	0.9 ± 0.3	1400 ± 1000
CCRF-CEM T-cells	**1**	2.0 ± 0.2	1.3 ± 0.2	3360

[a] See equation 2 for explanation of parameters. Data for conjugate **1** were calculated by fitting experimental data into eq. 2 using a fixed value of the parameter α as determined from data on nonspecific adsorption. Data for conjugates **2** and **7** were calculated using all variable parameters.

conjugates (P(GFLG)-NP-CB) to HSB-2 T-cells when compared to Raji B-cells (Table 1).

Influence of the Amount of Epitopes per Polymer Chain on the Binding

The Langmuir binding isotherms of P(GFLG)-NP-CB conjugates (**1** and **2**) containing different amounts of NP per polymer chain to Raji B-cells and HSB-2 T-cells were clearly different (not shown). Binding parameters obtained from the best fit are presented in Table 1. The parameter of nonspecific interactions α was a variable parameter during the fitting procedure. The conjugate **1** containing 20.8 wt.% NP (approximately four NP molecules attached per polymer chain) bound to the cell surface with an efficiency of about one order of magnitude higher when compared to conjugate **2** containing 6.8 wt.% NP (approximately one NP per polymer chain). Affinity constants were estimated assuming that all NP moieites in the conjugates were involved in ligand-receptor interactions. It is interesting to note that calculated values of the α parameters for conjugate **2** were also lower those of conjugate **1**.

Influence of the Spacer Structure on the Binding

The length of the spacer between the polymer backbone and the epitope could influence the biorecognition of the conjugate by cell surface receptors. Two HPMA copolymer conjugates were compared, namely P(GFLG)-NP-CB (conjugate **1**) and P(GG)-NP-CB (conjugate **7**). The Langmuir binding isotherms (not shown) of P(GG)-NP-CB (conjugate **7**) where the NP was coupled to the polymer backbone via a short dipeptide (GG) spacer possessed a considerably lower efficacy of binding to Raji B-cells and HSB-2 T-cells than P(GFLG)-NP-CB (conjugate **7**) as the calculated affinity constants indicate (Table 1).

The binding parameters were calculated using variable α parameters. The values of K_a for P(GG)-NP-CB (conjugate **7**) were 4–5 fold lower than the values for the P(GFLG)-NP-CB (conjugate **1**) for both Raji and HSB-2 cells (Table 1). Lower values of K_a for P(GG)-CB-NP (conjugate **7**) were observed in spite of the fact that its NP content (28.5 wt.%) was higher than in conjugate **1** (20.8 wt.%).

Cytotoxicity of Conjugates to T and B Lymphoblastic Cells

Free ADR, targeted conjugates **3** and **4** (P(GFLG)-NP-ADR) and non-targeted conjugate **6** (P(GFLG)-ADR) were assessed for their dose dependent growth inhibitory effect on Raji B-cells, CCRF-HSB-2 and CCRF-CEM T-cells in vitro. The values of the IC_{50} doses are listed in Table 2. As expected, the attachment of ADR to a non-targeted polymer carrier substantially decreased the cytotoxicity of ADR as a result of the limitation of cell uptake of the conjugate to the fluid-phase pinocytosis. The targeted conjugates, which enter cells by receptor-mediated pinocytosis, were considerably more toxic. The highest difference between the IC_{50} doses of non-targeted and targeted conjugates was obtained for HSB-2 T-cells (Table 2).

The comparison of the cytotoxicity of conjugates **3** and **4** demonstrated the influence of multivalent binding on biological properties. In agreement with the affinity constants of CB labeled conjugates **1** and **2** (Table 1), the conjugate **3** had a substantially lower IC_{50}. value than conjugate **4** (Table 2).

The internalization of conjugate **4** in Raji B-cells and in HSB-2 T cells was studied by confocal fluorescence microscopy. The images clearly indicate the internalization of the conjugate via the endocytic route (Fig. 4).

Accumulation of Conjugate 1 in Subpopulations of Peripheral Blood Lymphocytes

The accumulation of conjugate **1** in subpopulations of PBL was assessed. Preliminary experiments verified that the

Table 2. The IC_{50} Dose Values for Free and HPMA Copolymer-Bound ADR

Cells	Free ADR μM	Conjugate **3** μM	Conjugate **4** μM	Conjugate **6** μM
CCRF-HSB-2	0.005	0.3	0.6	7
CCRF-CEM	0.009	0.7	1.0	8
Raji	0.062	5.3	7.7	42

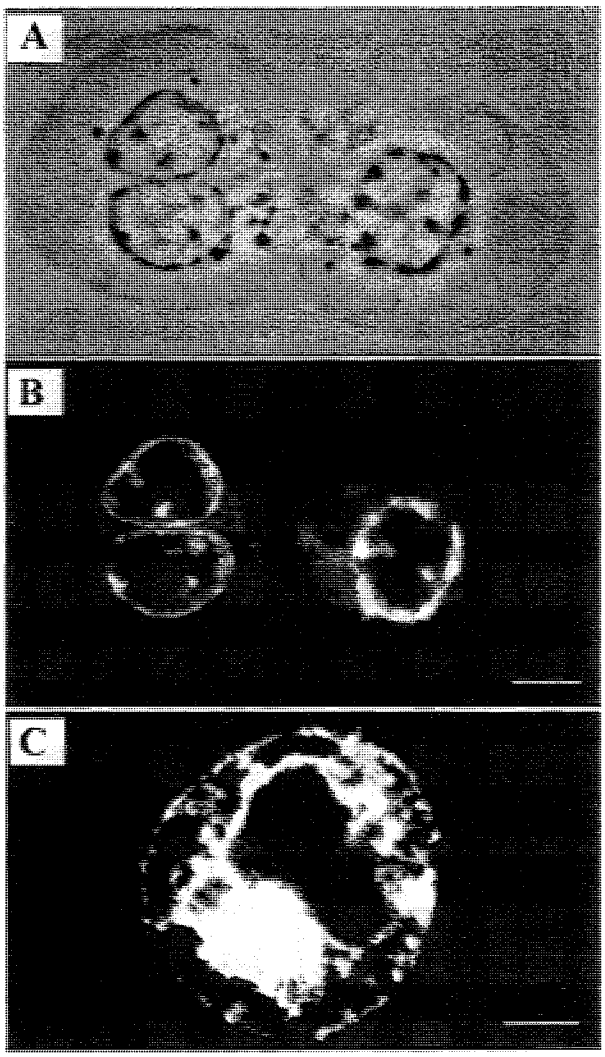

Fig. 4. Localization of conjugate **4** in Raji B cells (A-contrast phase image; B-fluorescent image) and fluorescent image in HSB-2 T-cells (C) as determined by confocal fluorescence microscopy; bar 5 μm.

conjugate was not cytotoxic toward CEM and Raji cells during 72 h of incubation. We assumed that CB, due to its negative charge would remain inside the cells during the time of the experiment.

The PBL cells were incubated with the conjugate for 72 h at 37°C. After incubation they were divided into three portions and separately stained by B and T cell specific antibodies. B lymphocytes, a whole population of T lymphocytes, and a subpopulation of helper/inducer T cells were stained with anti-CD19, anti-CD3, and anti-CD4 mouse antibodies, respectively. The results (not shown) demonstrated that the conjugate was accumulated in all three subpopulations of PBL. The relative accumulation was larger in T cells ($CD3^+$ cells > $CD4^+$ cells) when compared to B cells ($CD19^+$ cells).

Toxicity of Conjugate 3 to Peripheral Blood Lymphocytes

Varying concentrations of conjugate 3 were incubated with fresh PBL cells in RPMI medium for 72 h. Equal aliquots of cell suspensions were taken for the incubation with the conjugate and for control experiments. Cells were once washed with DPBS, transferred into an equal volume of DPBS (0.5 ml), and analyzed by flow cytometry. The cytotoxicity of the conjugate was assessed in two ways: the estimation of the amount of viable cells according to their shape and size, and by the estimation of the fraction of apoptotic cells.

The flow cytometry analysis of PBL cells incubated with conjugate **3** at the concentration of 20 μM ADR equivalent is shown on Fig. 5 A,B. The lymphocytes were gated by their 'scatter morphology'. The light scatter histogram of control lymphocytes is presented in the left panel of the Fig. 5A. On the right panel of the Fig. 5A there is the histogram of PBL cells incubated with conjugate **3**. The data seem to indicate that 98% of cells exposed to conjugate **3** possessed scatter parameters similar to control cells. It may suggest that 98% of cells were viable after the treatment.

In Fig. 5B a two-color analysis, for ADR and Annexin V-FITC fluorescence, is presented. Staining of cells with Annexin V-FITC showed that about 2.5% of control cells were in an apoptotic state after 72 h of incubation (Fig. 5B, left panel). After incubation of PBL cells with conjugate **3** (20 μM ADR equivalent) for 72 h, the amount of cells in apoptotic state was unchanged (Fig. 5B, right panel). However, 33% of cells were positive for ADR fluorescence. It is interesting that the fraction of cells containing ADR was significantly higher than the fraction of cells in the apoptotic state.

Cytotoxicity of Conjugate 3 to HSB-2 T Cells

A similar approach, as described above for PBL cells, was used for HSB-2 cells. The HSB-2 cells were incubated with conjugate **3** (20 μM ADR equivalent) for 72 h at 37°C. The flow cytometer analysis of control HSB-2 cells is presented in the Fig. 6A (left panel). The light scatter parameter analysis of the cells incubated with conjugate **3** showed that only about 0.4% of cells possessed light scatter parameters, which were similar to the parameters of control cells (Fig. 6A, right panel). Most of cells were fragmented as seen from changes of the light scatter parameters. It is worth to note that the flow cytometer approach for evaluation of the cell viability appeared to be more feasible and sensitive for a suspension of cells than the MTT assay. Although the use of the MTT assay is rapid and precise, we found that care should be taken when using this assay for short-term cytotoxicity assays since non-viable cells also reduce the tetrazolium dye.

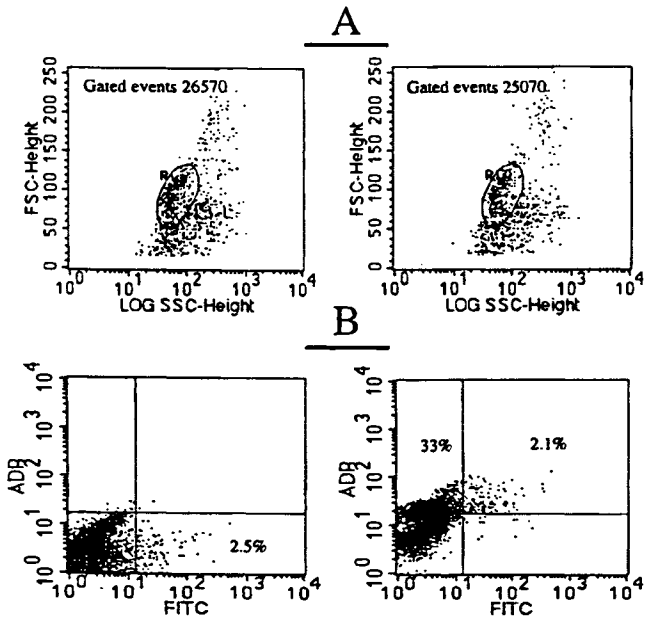

Fig. 5. Representative flow cytometry analysis of viability and development of apoptosis in PBL cells incubated with conjugate **3** (20 μM of ADR equivalent) at 37°C for 72 h. The ApoAlert™ Annexin V/PI kit was used to monitor the early stage of apoptosis. The lymphocytes were gated by their 'scatter morphology'. The 'gate' marked as the area "R". Time interval of accumulation of data was equal for both control and experiment runs. (A) The light scatter histograms of control cells (left panel) and cells incubated with conjugate (right panel). (B) Two-color flow cytometry analysis (ADR and FITC-Annexin fluorescence). Left panel-control cells; right panel-incubated cells).

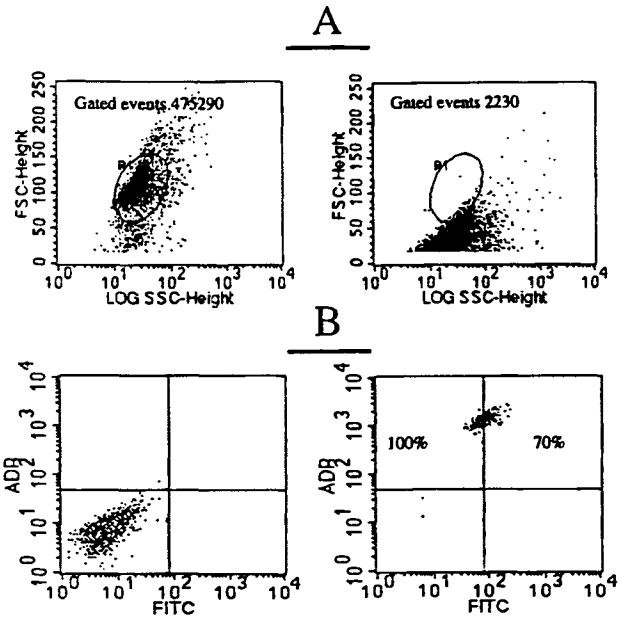

Fig. 6. Representative flow cytometry analysis of viability and development of apoptosis in HSB-2 cells incubated with conjugate **3** (20 μM of ADR equivalent) at 37°C for 72 h. See Fig. 5 for explanation.

A two-color flow cytometry analysis (ADR and Annexin V-FITC fluorescence) was performed (Fig. 6B). The analysis showed that 100% of cells, which were still viable according to the flow cytometer analysis contained ADR and about 70% of them were stained with Annexin V-FITC (Fig. 6B, right panel). The latter indicates that though the cells had unchanged size and shape they were already in an apoptotic state. In other words, the percent of surviving cells at the end of the incubation period was lower than 0.4 %.

The dose dependence of the viability HSB-2 T cells and PBL cells were compared. Concentrations of conjugate **3**, which have eradicated more than 99% of HSB-2 T lymphoblastic cells were not toxic to PBL cells.

DISCUSSION

The CD21 (CR2) receptor is an 145 kDa integral transmembrane single-chain glycoprotein that recognizes the C3dg fragment of the human complement factor C3 (21) and the EBV receptor with the ligand localized in the NP sequence of the gp350/220 envelope glycoprotein (13). The CD21 receptor is expressed on B-lymphocytes (13,22) and on peripheral T lymphocytes (23,24). About 50% of the peripheral blood $CD8^+$ T cell subpopulation can bind the EBV (25). It appears that this receptor is overexpressed on B and T lymphoblastoid cells (12,26).

The EBV seems to bind to both Raji B-cells (13) and CCRM-HSB-2 T-cells (24). However, a different picture was obtained with microspheres containing covalently attached NP. Only a portion of Raji B-cells (47–76%) and about 11% of HSB-2 T-cells were stained (13). On the other hand, we have observed by flow cytometry (Fig. 2) a homogeneous binding of HPMA copolymer conjugates to B- and T-cells. These facts seem to indicate that a multivalent, flexible macromolecular NP conjugate may possess a potential as a targetable drug delivery system. The aim of this study was to evaluate the biorecognition of HPMA copolymers containing covalently attached NP (EDPGFFNVE) by T and B lymphocytes. One B-cell line (Raji) and two T-cell lines (CCRM-CEM and CCRM-HSB-2) were chosen for the study.

The design of the conjugates (Fig. 1) permitted to evaluate the influence of the amount of NP per polymer chain as well as the structure of the oligopetide side-chain on the biorecognizability. Conjugates **1** and **2** contained a different amount of GFLGEDPGFFNVE side-chains, whereas conjugates **1** and **7** differed in their structure. The latter contained GGEDPGFFNVE side-chains. Conjugates **3** and **4** contained ADR in addition to NP. This permitted to correlate the biorecognition of the conjugates at the cell surface (Table 1) with the cytotoxicity (Table 2) of the intracellularly released ADR after internalization of the conjugate by receptor-mediated endocytosis (Fig. 4).

The data obtained indicated specific binding of the NP-containing conjugates to all three cell lines studied. At concentrations corresponding to approximately 50 μM of NP equivalent (about 180 μg/ml of conjugates) the binding sites of Raji B-cells and HSB-2 and CEM T-cells were saturated with conjugates. Following saturation of binding sites, the conjugates nonspecifically adsorbed to the cell surface. The amount of nonspecific binding was proportional to the concentration of the conjugate, but considerably lower than the specific binding. The estimated apparent affinity constants, K_a, and the amount of the conjugates bound to the cells at saturation were different for B-cells and T-cells (Table 1). The analysis performed was limited due to the unknown number of NP moieties involved in biorecognition. We assumed that all NP moieties bound to HPMA copolymer chains were involved in interactions with receptors. Due to the flexibility of the HPMA copolymer the assumption may be close to reality.

Surprisingly, the estimated K_a value for CEM and HSB-2 T-cells was approximately two fold higher when compared to the K_a value obtained for Raji B-cells (Table 1). One of the explanations could be the difference in the density of receptors on the cell surface. Estimation of the number of receptors saturated with conjugates revealed that Raji B-cells have about 70,000 receptors per cell whereas the CEM and HSB-2 T-cells have about two times less receptors. On the other hand, the size of Raji B-cells is 1.2–1.3 larger than that of CEM and HSB-2 T-cells resulting in an 1.4 to 1.7 times larger surface area. Consequently, the density of receptors on all cell lines is similar. Apparently the difference in the binding affinity of conjugates to B- and T-cells can not be explained by a difference of the density of receptors on the cell surface.

Polymeric chains containing several ligands could interact with cells in a multipoint attachment mode. Indeed a cooperative effect seems to be operative. Conjugate **1** which contained about 4 NP moieties per chain possessed an one order of magnitude better binding affinity when compared to conjugate **2** which contained about 1 NP moiety per chain (Table 1). These data are in agreement with the literature. It was observed that efficient binding of the N-terminal gp350/220 peptide to CD21 receptor requires presentation as a multivalent ligand (13).

The evaluation of the cytotoxicity of conjugates in vitro has shown that attachment of ADR to a nontargeted conjugate **6** resulted in a substantial increase in the IC_{50} dose when compared to free ADR (Table 2). This expected fact (1) reflects the change in the mechanism of cell entry (fluid-phase pinocytosis vs. free diffusion) resulting in altered intracellular drug concentrations. Targeted conjugates **3** and **4**, P(GFLG)-NP-ADR, which enter cells by receptor-mediated pinocytosis, were found to be much more toxic. It is reasonable to assume that the rate of release of ADR from the HPMA copolymer chains in the lysosomal compartments (15,16) are similar for targeted and non-targeted conjugates. Then the ratio of the IC_{50} values of non-targeted to targeted conjugates could be used as an estimate of the targetability of conjugates containing the NP. The data indicated (Table 2) that the highest difference between the cytotoxicity of targeted conjugates **3** and **4** on one hand and the non-targeted conjugate **6** on the other was found in HSB-2 T cells. This is in agreement with the binding studies. The affinity of CB containing conjugates **1** and **2** to HSB-2 T cells was almost two times higher than that to Raji B cells (Table 1).

The structure of the side-chain has also an impact on the biorecognition. The P(GG)-NP-CB conjugate **7** containing the NP attached via the GG dipeptide possessed an almost five fold lower affinity for both B- and T-cells when compared to the P(GFLG)-NP-CB conjugate **1** with a spacer composed of the tetrapeptide (GFLG). Two possible explanations are obvious. Sterical hindrance by polymer chains may render the biorecognition of the NP by the CD21 receptor more difficult when a short GG spacer was placed between the HPMA copolymer backbone and the NP. Similar sterical hindrance effects were

observed in the interactions of enzyme active sites with oligopeptide side-chains attached to HPMA copolymers (15,16). On the other hand, different spacers result in different epitopes, GFLGEDPGFFNVE in conjugates **1** and **2**, and GGEDPGFFNVE in conjugate **7**. It was suggested that in addition to CD21, there are other cell membrane receptors to which EBV can bind on T-cells (27,28). This may be also the case with the HPMA copolymer conjugates.

We demonstrated that the NP-containing HPMA copolymer (conjugate **1**) interacts with PBL. According to the flow cytometry analysis, both B and T lymphocytes accumulated the P(GFLG)-NP-CB conjugate. Quantitative analysis and comparison of accumulation of the conjugate in various T and B lymphoblastic cells as well as in subpopulation of PBL should be done in order to obtain a more precise picture of distribution of receptors for the NP.

It is very interesting to note that conjugate **3** at a concentration, which was lethal for T lymphoblastic cells, was not toxic for PBL. At the same time, the percentage of PBL cells in the apoptotic state was unchanged after incubation with conjugate **3**, when compared to control cells. About one third of PBL cells contained ADR, but after 72 h incubation with the conjugate, the accumulated amount of ADR was not sufficient to trigger apoptosis. For example, at a concentration of conjugate equal to 20 μM of ADR equivalent, the ADR fluorescence of HSB-2 T cells was about 100 fold higher than that of PBL cells. The different rate of ADR uptake is consistent with the expression of EBV receptors. The amount of EBV receptors on T lymphocytes was about 10 and 50 times less than the amount on malignant Molt-4 T cells and Raji B-cells, respectively (29).

In summary, the data seem to indicate the potential of using small synthetic receptor binding epitopes as targeting moieties for polymer based targetable drug delivery systems. The relatively small size of the conjugates should possess only a minor hindrance to transport across transcompartmental barriers. In addition, attachment of numerous ligands per polymer chain, without impairing the solubility of the conjugate, permits the design of conjugates with a high binding affinity. Preliminary data on an in vivo mouse model seem to support our conclusions (30).

ACKNOWLEDGMENTS

We thank Dr. Blanka Říhová for valuable discussions.

REFERENCES

1. D. Putnam and J. Kopeček. Polymer conjugates with anticancer activity. *Adv. Polym. Sci.* **122**:55–123 (1995).
2. H. Maeda, L. M. Seymour, and Y. Miyamoto. Conjugates of anticancer agents and polymers: Advantages of macromolecular therapeutics in vivo. *Bioconjugate Chem.* **3**:351–362 (1992).
3. R. Duncan, L. C. W. Seymour, L. Scarlett, J. B. Lloyd, P. Rejmanová, and J. Kopeček. Fate of N-(2-hydroxypropyl)methacrylamide copolymers with pendent galactosamine residues after intravenous administration to rats. *Biochim. Biophys. Acta* **880**:62–71 (1986).
4. B. Říhová, P. Kopečková, J. Strohalm, P. Rossmann, V. Větvička, and J. Kopeček. Antibody directed affinity therapy applied to the immune system: in vivo effectiveness and limited toxicity of daunomycin conjugated to HPMA copolymers and targeting antibody. *Clin. Immunol. Immunopathol.* **46**:100–114 (1988).
5. V. Omelyanenko, P. Kopečková, C. Gentry, J.-G. Shiah, and J. Kopeček. HPMA copolymer-anticancer drug-OV-TL16 antibody conjugates. 1. Influence of the methods of synthesis on the binding affinity to OVCAR-3 ovarian carcinoma cells in vitro. *J. Drug Target.* **3**:357–373 (1996).
6. G. B. Sigal, M. Mammen, G. Dahman, and G. M. Whitesides. Polyacrylamides bearing pendant sialoside groups strongly inhibit agglutination of erythrocytes by influenza virus: The strong inhibition reflects enhanced binding through cooperative polyvalent interactions. *J. Am. Chem. Soc.* **118**:3789–3800 (1996).
7. R. C. Rathi, P. Kopečková, and J. Kopeček. Biorecognition of sugar containing N-(2-hydroxypropyl)methacrylamide copolymers by immobilized lectin. *Macromol. Chem. Phys.* **198**:1165–1180 (1997).
8. A. V. Tersikh, J.-M. Le Doussal, R. Crameri, I. Fisch, J.-P. Mach, and A. V. Kajava, "Peptabody": A new type of high avidity binding protein. *Proc. Natl. Acad. Sci. USA* **94**:1663–1668 (1997).
9. R. K. Jain, Delivery of novel therapeutic agents in tumors: physiological barriers and strategies. *J. Natl. Cancer Inst.* **81**:570–576 (1989).
10. N. L. Krinick, Y. Sun, D. Joyner, J. D. Spikes, R. C. Straight, and J. Kopeček. A polymeric drug delivery system for the simultaneous delivery of drugs activatable by enzymes and/or light. *J. Biomat. Sci., Polym. Ed.* **5**: 303–324 (1994).
11. J.-G. Shiah, Y. Sun, P. Kopečková, M. Peterson, and J. Kopeček. Biodistribution in tumor bearing mice of free and HPMA copolymer-bound meso-chlorin e_6 and adriamycin. 25th Int. Symposium on Controlled Release of Bioactive Materials, Las Vegas, Nevada, June 21–24, 1998. Proceedings, pp. 95–96.
12. S. K. Hobs, W. L. Monsky, F. Yuan, W. G. Roberts, L. Griffith, V. P. Torchilin, and R. K. Jain. Regulation of transport pathways in tumor vessels: Role of tumor type and microenvironment. *Proc. Natl. Acad. Sci. USA* **95**:4607–4612 (1998).
13. G. R. Nemerow, R. A. Houghten, M. D. Moore, and N. R. Cooper. Identification of an epitope in the major envelope protein of Epstein-Barr virus that mediates viral binding to the B lymphocyte EBV receptor (CR2). *Cell* **56**:369–377 (1989).
14. D. Watry, J. A. Hedrick, S. Siervo, G. Rhodes, J. J. Lamberti, J. D. Lambris, and C. D. Tsoukas. Infection of human thymocytes by Epstein-Barr virus. *J. Exp. Med.* **173**:971–980 (1991).
15. J. Kopeček and P. Rejmanová. Enzymatically degradable bonds in synthetic polymers. In S. D. Bruck (ed.), *Controlled Drug Delivery*, CRC Press, Boca Raton, Florida, 1983, vol. I, pp. 81–124.
16. P. Rejmanová, J. Pohl, M. Baudyš, V. Kostka, and J. Kopeček. Polymers containing enzymatically degradable bonds. 8. Degradation of oligopeptide sequences in N-(2-hydroxypropyl)methacrylamide copolymers by bovine spleen cathepsin B. *Makromol. Chem.* **184**:2009–2020 (1983).
17. J. Kopeček. Synthesis of tailor-made soluble polymeric carriers. In J. M. Anderson, S. W. Kim (eds.), *Recent Advances in Drug Delivery Systems*, Plenum Press, New York, NY, 1984, pp. 41–62.
18. M. B. Hansen, S. E. Nielsen, and K. Berg. Re-examination and further development of a precise and rapid dye method for measuring cell growing/cell kill. *J. Immunol. Meth.* **119**:203–210 (1989).
19. G. C. Salzman, J. M. Growell, J. C. Martin, *et al.* Cell identification by laser light scattering: Identification and separation of unstained leukocyte. *Acta Cytol. (Praha)* **19**:374–377 (1975).
20. I. Vermes, C. Haanen, H. Steffens-Nakken, and C. Reutelingsperger. A novel assay for apoptosis. Flow cytometric detection of phosphatidylserine expression on early apoptotic cells using labeled Annexin V. *J. Immun. Methods* **184**:39–51 (1995).
21. J. D. Lambris, V. S. Ganu, S. Hirani, and H. J. Muller-Eberhard. Mapping of the C3d receptor (CR2)-binding site and a neoantigenic site in the C3d domain of the third component of complement. *Proc. Natl. Acad. Sci. U.S.A.* **82**:4235–4239 (1985).
22. J. Tanner, J. Weis, D. Fearon, Y. Whang, and E. Kieff. Epstein-Barr virus gp350/220 binding to the B lymphocyte C3d receptor mediates adsorption, capping, and endocytosis. *Cell* **50**:203–213 (1987).
23. C. D. Tsoukas and J. D. Lambris. Expression of EBV/C3d receptors on T cells. *Immunology Today* **14**:56–59 (1993).
24. E. Fischer, C. Delibrias, and M. D. Kazatchkine. Expression of CR2 (the C3dg/EBV receptor, CD21) on normal human peripheral blood T lymphocytes. *J. Immunol.* **146**:865–869 (1991).

25. G. Sauvageau, R. Stocco, S. Kasparian, and J. Menezes. Epstein-Barr virus receptor expression on human CD8+ (cytotoxic/suppressor) T lymphocytes. *J. Gen. Virol.* **71**:379–386 (1990).
26. R. Rask, J. M. Rasmussen, H. V. Hansen, P. Bysted, and S. E. Svehag. Complement C3dg/Epstein-Barr virus receptor density on human B lymphocytes estimated by immunoenzymatic assay and immunocytochemistry. *J. Clin. Lab. Immunol.* **25**:153–156 (1988).
27. J. A. Hedrick, D. Watry, C. Speiser, P. O'Donnell, J. D. Lambris, and C. D. Tsoukas. Interaction between Epstein-Barr virus and a T cell line (HSB-2) via a receptor phenotypically distinct from complement receptor type 2. *Eur. J. Immunol.* **22**:1123–1131 (1992).
28. R. Stocco, G. Sauvageau, and J. Menezes. Differences in Epstein-Barr virus (EBV) receptors expression on various human lymphoid targets and their significance to EBV-cell interactions. *Virus Res.* **11**:209–225 (1988).
29. I. Muller, A. Jenner, G. Bruchelt, D. Niethammer, and B. Halliwell, Effect of concentration on the cytotoxic mechanism of doxorubicin-apoptosis and oxidative DNA damage. *Biochem. Biophys. Res. Commun.* **230**:254–257 (1997).
30. R. K. Prakash, C. M. Clemens, C. D. Ebert, V. Omelyanenko, P. Kopečková, and J. Kopeček. Targeting of macromolecular prodrugs to T-lymphocytes. *24th Intern. Symp. Contr. Rel. Bioact. Mater.*, July 15–19, 1997 Stockholm, Sweden; Proceedings, pp. 859–860.